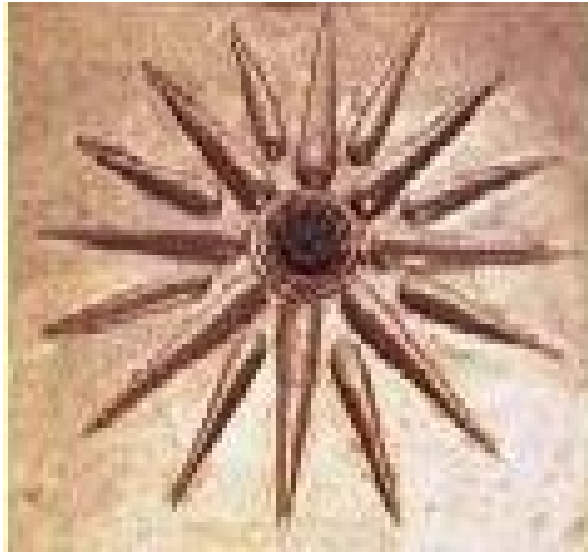


**Test beam data analysis**  
**for CASTOR**  
**CMS forward calorimeter**



**Agni Bethani**  
**(National Technical University of Athens)**



**DESY summer students program 2008**



# Table of Content

## Introduction

- CMS experiment and CASTOR
- Physics with CASTOR
- CASTOR detector
- Calorimeter description

## Test beam analysis

- Pedestal analysis
- Electron energy scan: beam counters study
- LED analysis

## Conclusions

## References

# Introduction

## *CMS experiment and CASTOR*

CMS (compact muon solenoid) is one of the two large multipurpose experiments at the Large Hadron Collider (LHC) at CERN. The Compact Muon Solenoid (CMS) is a general-purpose detector designed to exploit the physics of p-p collisions at the centre-of-mass energy of 14 TeV over the full range of luminosities expected at the LHC. The CMS is capable to study aspects of heavy ion collisions as well. The CMS detector is designed to measure the energy and momentum of photons, electrons, muons, and other charged particles with high precision, resulting in an excellent mass resolution for many new particles.

The CASTOR detector is a part of this huge experiment and along with Totem-T2 tracking detector in front of CASTOR is a complete unit producing data that can be studied independently of the rest of CMS. CASTOR is located in the very forward region of CMS, 14.38 m from the interaction point (IP5), covering the pseudorapidity range  $5.2 < \eta < 6$  and it will extend the CMS pseudorapidity range to a total of about 11.5  $\eta$ -units, being only on one side of the IP.

## *Physics with CASTOR*

The original motivation for CASTOR (Centauro And Strange Object Research) was to study in the laboratory, using heavy-ion beams from the LHC, unexplained phenomena seen in cosmic rays. The LHC will be the first accelerator to effectively probe the very high energy cosmic ray domain, close to the end of the cosmic ray spectrum. Both experimental data and model predictions indicate that the forward rapidity region is the most favorable place for the production and detection of the exotic cosmic ray phenomena. Favorable conditions for exotic event productions are expected in the pseudorapidity region  $5 < \eta < 7$ .

The physics program for CASTOR as part of CMS now goes beyond the study of cosmic ray phenomena and will be used in both pp and HI physics in general. It will provide information on the following topics:

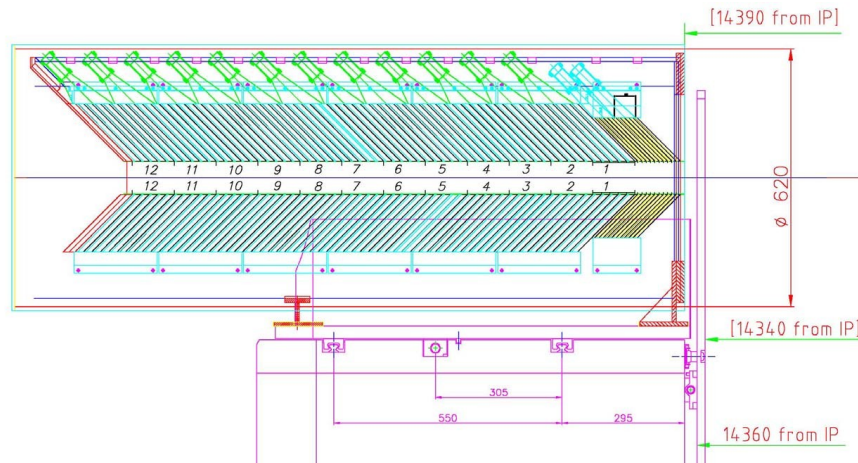
- Cosmic- ray Centauros and strangelets
- beyond standard model physics
- Higgs physics
- Multi-Parton Interactions and Underlying event structure
- Low-x QCD physics
- Diffractive QCD
- Quark-Gluon-Plasma

## CASTOR detector

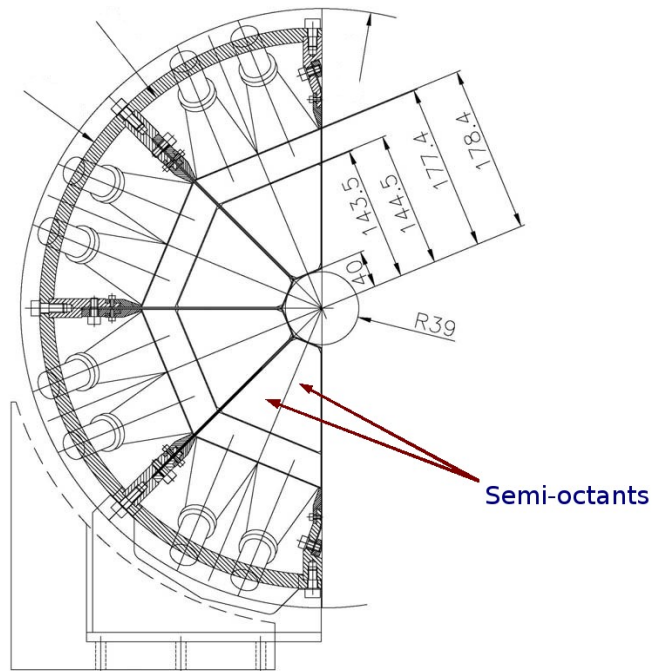
The CASTOR detector is an electromagnetic (EM) and a hadronic (HAD) calorimeter azimuthally symmetric around the beam pipe. It consists of 16 azimuthal semi-octants. It is also longitudinally segmented into 14 sections, 2 for the EM and 12 for the HAD part. The calorimeter is constructed in layers of tungsten (W) plates as absorber and fused silica quartz (Q) plates as active medium. The signal is the Cherenkov light produced by the passage of the charged particles in the shower through the quartz medium.

### Calorimeter description

The calorimeter has 16x14 subdivisions (224 channels in total). The electromagnetic section has 2x16 channels and depth  $2 \times 10 = 20$  radiation lengths,  $X_0$ . For hadrons its depth corresponds to 0.77 interaction lengths,  $\lambda$ . Each channel (read out unit RU) consists of 5 tungsten and 5 quartz plates of thickness 5 mm and 2 mm respectively. The hadronic section has 12x16 channels and depth  $12 \times 0.77 = 9.24\lambda$ . Each RU consists of 5 tungsten and 5 quartz plates of thickness 10mm and 4 mm respectively. The calorimeter has total depth  $10\lambda$ . The W/Q layers are inclined at  $45^\circ$  to the beam direction in order to efficiently capture the Cherenkov light. The index of refraction of quartz is  $n = 1.46 - 1.55$  for wavelengths  $\lambda = 600 - 200\text{nm}$ . The corresponding Cherenkov threshold velocity is  $\beta = 1/n = 0.65 - 0.69$  and therefore for  $\beta \sim 1$  the angle of emission is  $\theta = \arccos(1/\beta) = 46^\circ - 50^\circ$ . This angle also makes the detector insensitive to particles coming from rear caused by beam-gas collisions from beams packets passing through CASTOR on the way to the interaction point. The light produced in each channel is collected and focused by air-core light guides onto the corresponding PMTs.



The calorimeter is constructed in two semi-circular sections of 4- octants each, in order to be positioned around the fixed beam pipe. The final inner radius of the calorimeter has been set to 40mm, providing a distance of 2.5mm for misalignments and displacements.



Advantages of the calorimeter:

- Very fast response and signal duration of  $O(10\text{nsec})$
- Signal produced by charged particles with velocity above a threshold, thus the calorimeter is insensitive to induced radiation and soft neutrons
- The calorimeter works as a shower core detector and thus the hadronic showers have very small visible transverse size
- Radiation hardness of the materials
- Compact detector dimensions

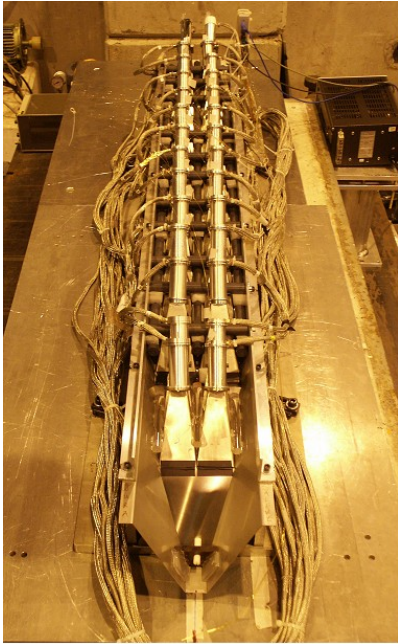
Disadvantages of the calorimeter :

- Non compensating calorimeter

# Test Beam analysis

## *CASTOR prototype*

Beam tests were carried out with the final CASTOR prototype using beams of electrons, pions and muons in different energies. The CASTOR prototype consists of two semi-octants, Jura and Saleve with 2 EM and 12 HAD channels each.



In our analysis the mapping of the channels is as follows:

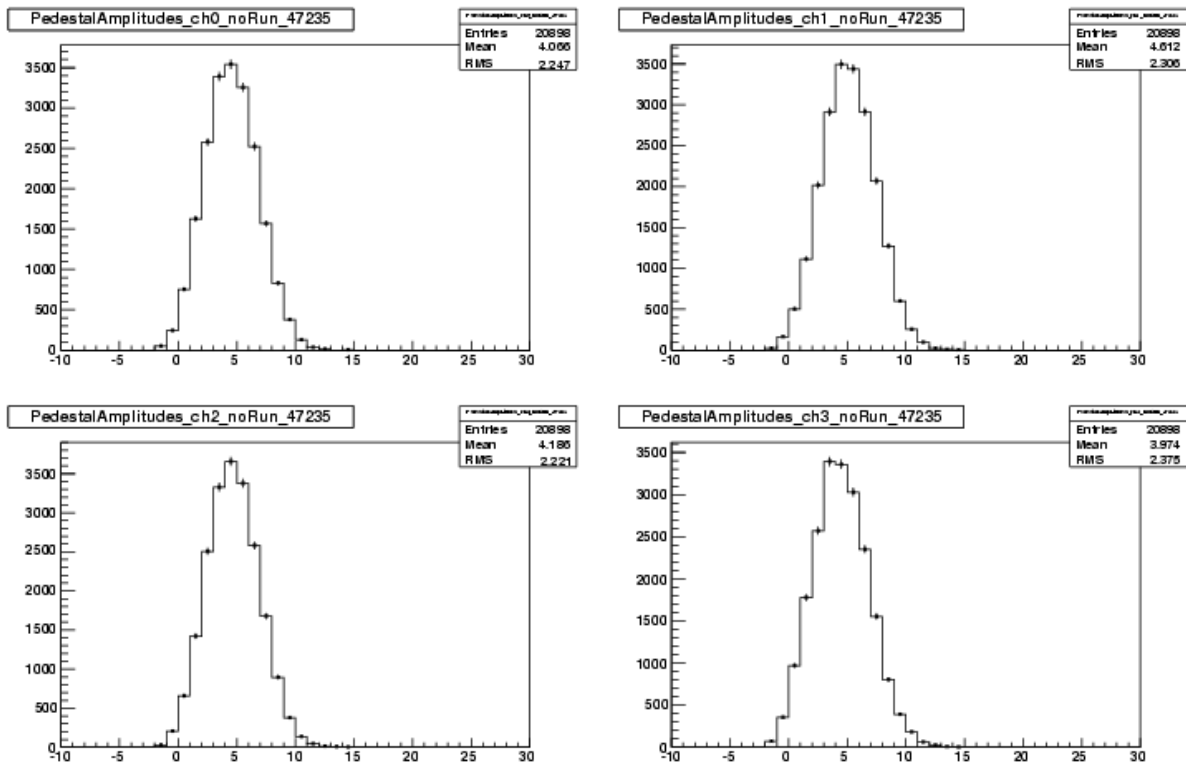
- Saleve side channels:0-13
- Jura side channels:14-27
- EM:0,1,14,15
- HAD:2-13,16-27

Channels 26, 27 had no input signal connected.

## Pedestal analysis

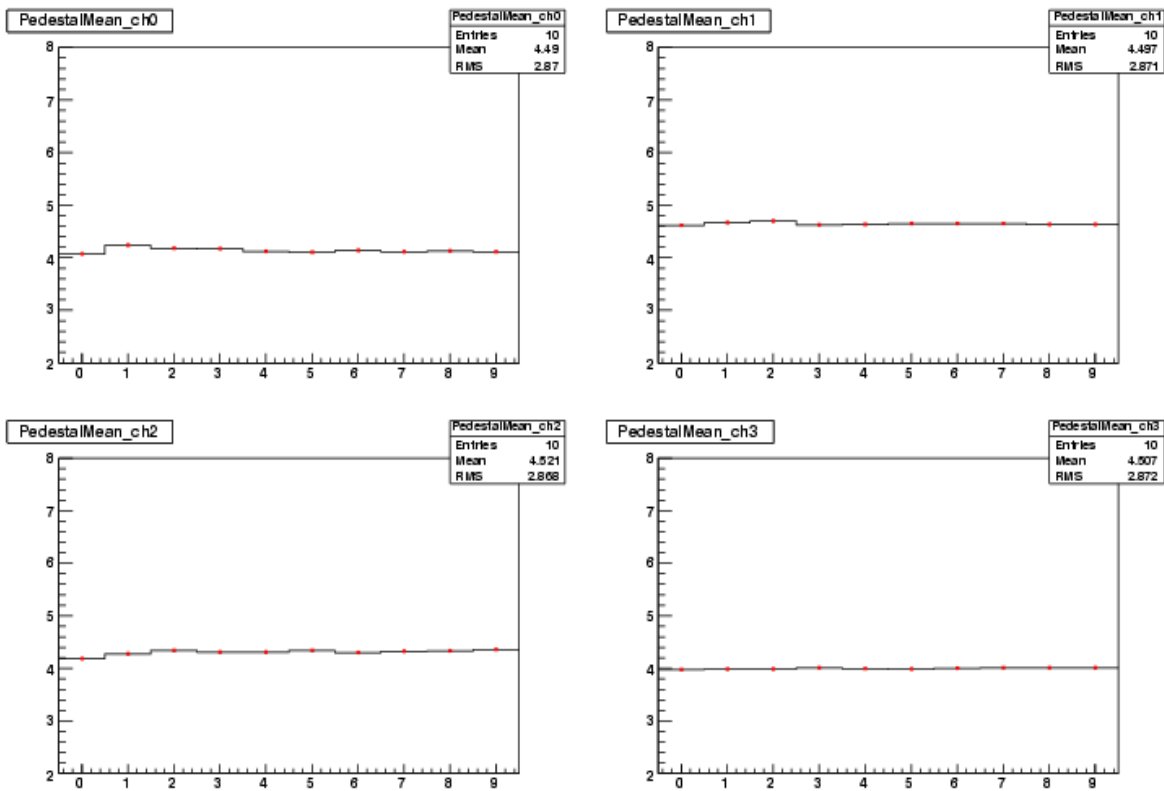
- Pedestal amplitudes

Electronics noise causes offset of reconstructed amplitudes (pedestal amplitudes). In the first part of the analysis the pedestal amplitude distributions are studied. The pedestal value is the sum of the amplitudes over 4 (out of 20) time slices for pedestal trigger events. We studied the time slices 3-6 and 16-19 and we got consistent results. The procedure was repeated for 10 different test-runs. In the following histograms the amplitude distributions for run no47235 (350 GeV pions, 2 faulty channels) observed for the first four saleve-side channels are presented. We prepared similar histograms for every run and every channel. In the graphs one can notice a Gaussian amplitude distribution that is common for all the channels.



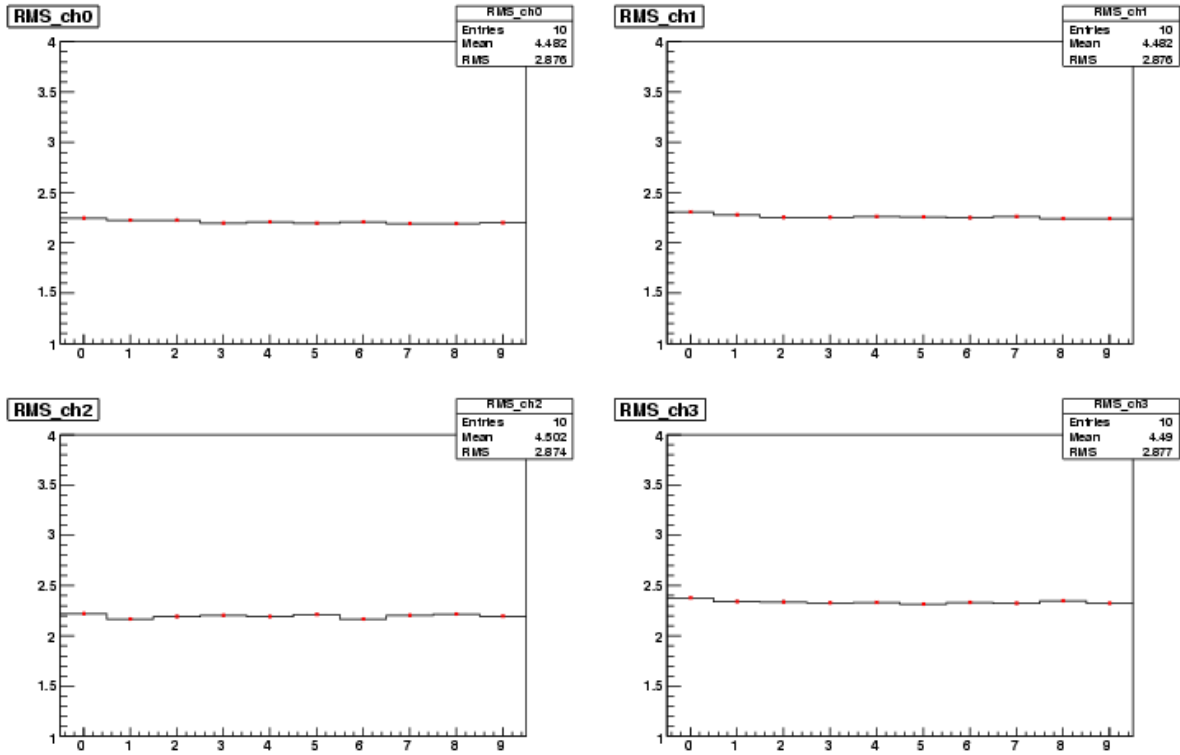
- Pedestal mean stability

For estimating the mean stability the mean value of the pedestal amplitude distribution for 10 different test runs were compared. The runs studied are 47235(pions),47440(pions) and 48514-48656(electron energy scan runs). The following histograms show the mean value for the 10 runs for the first 4 saleve-side channels. The mean value is obviously stable for each channel to a fraction of a count.



- Pedestal RMS stability

In addition to the mean value stability we examined the respective RMS stability. The RMS values are also stable as shown in the following histograms.



Therefore the overall conclusion is that the behavior of the electronics is stable throughout test beam.

## Electron energy scan: beam counters study

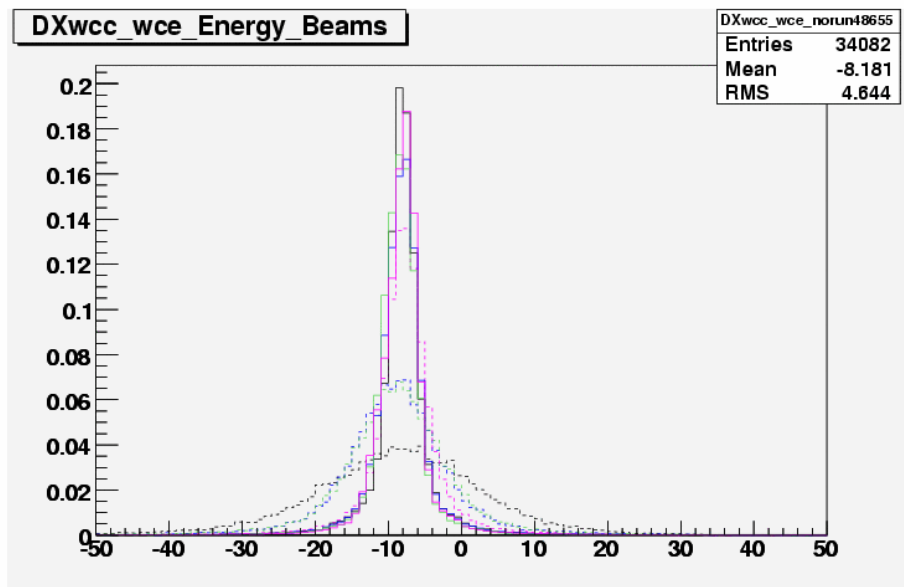
The purpose of this analysis is to examine the behavior of the beam counters for electron beams of different energies. For all cases we requested beam trigger events. In the case of the wire chambers we also requested single hit events along either the x or y axis.

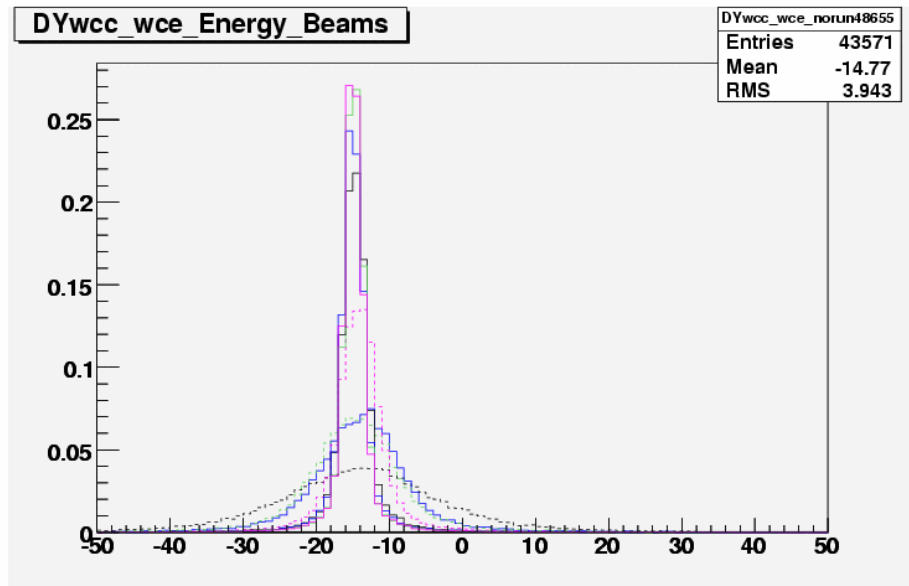
In the following histograms, every run is depicted by the same type of line as described below:

Dashed: 10 GeV(black), 20 GeV(blue, green ), 50 GeV(magenta)  
Solid: 120 GeV(black), 150 GeV(blue), 180 GeV(green ), 200 GeV(magenta)

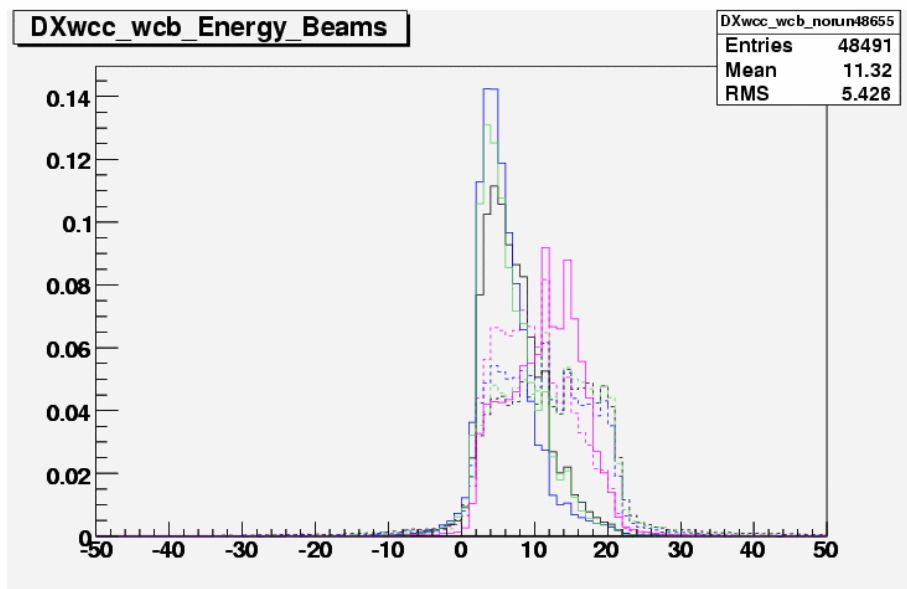
- *Wire chambers: B, C and E*

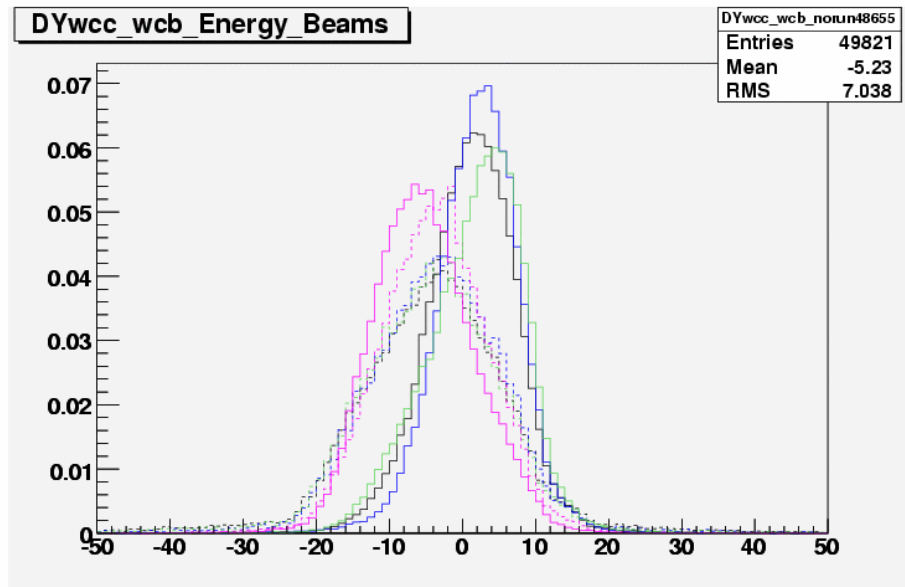
We studied the differences in the wire chamber position reconstruction. Specifically we compare the wire chambers two by two. Firstly we compare the wire chambers C and E along the x and y axis respectively. One can notice the Gaussian distribution of the differences in position. In addition we see that the distribution is wider for lower energies.



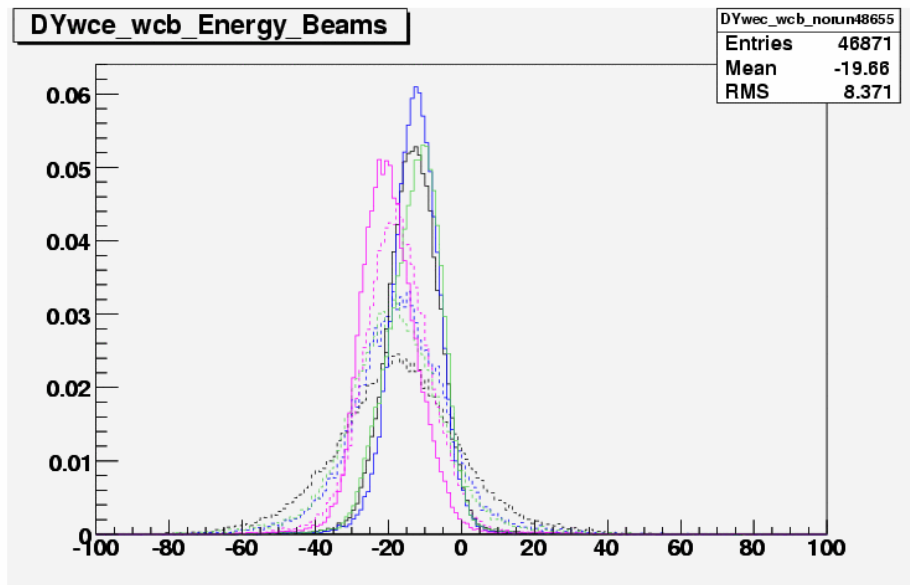
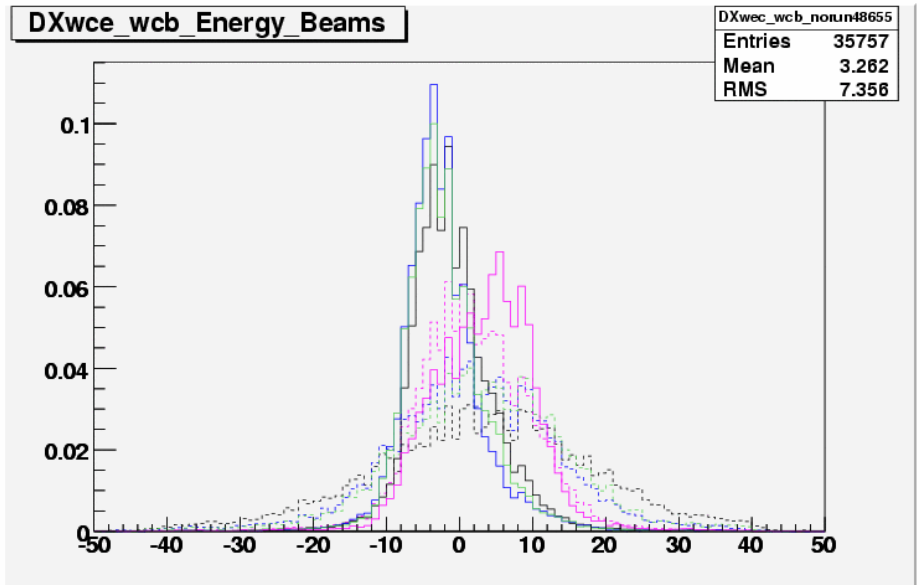


However, comparing the wire chambers C and B we can see, apart from a wider distribution, a shift to higher values for the x axis and to lower values for the y axis for the lower energy beams. In addition the shape is not Gaussian for this runs anymore. The 200GeV beam also shows the same behavior.



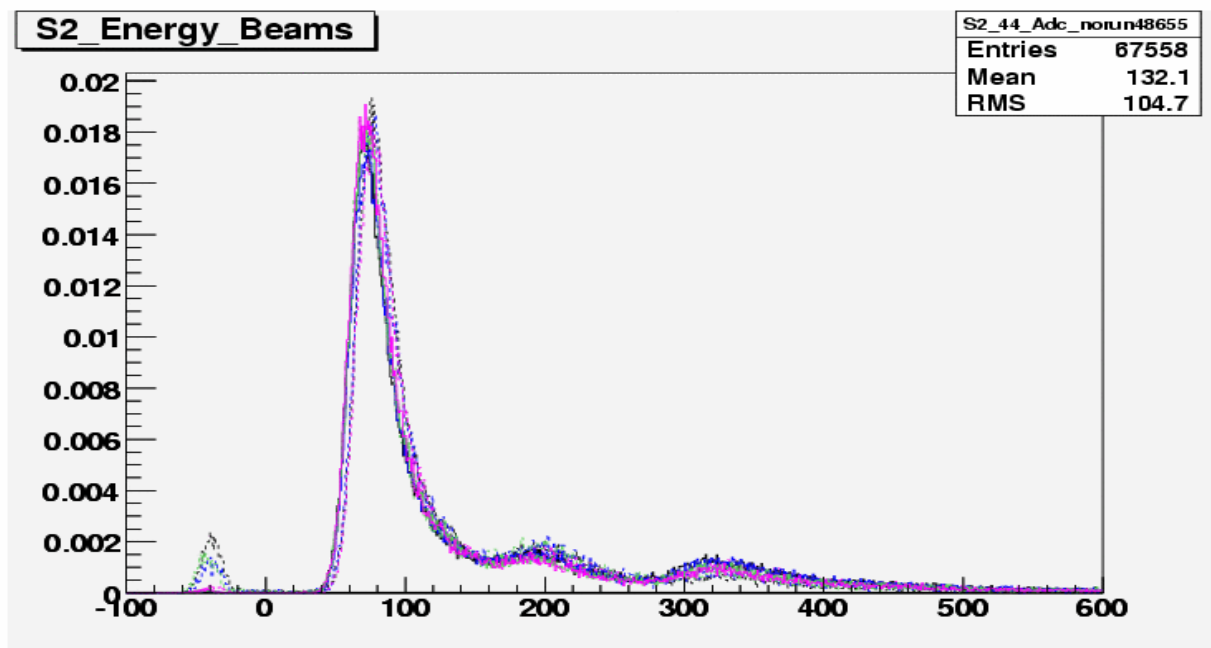
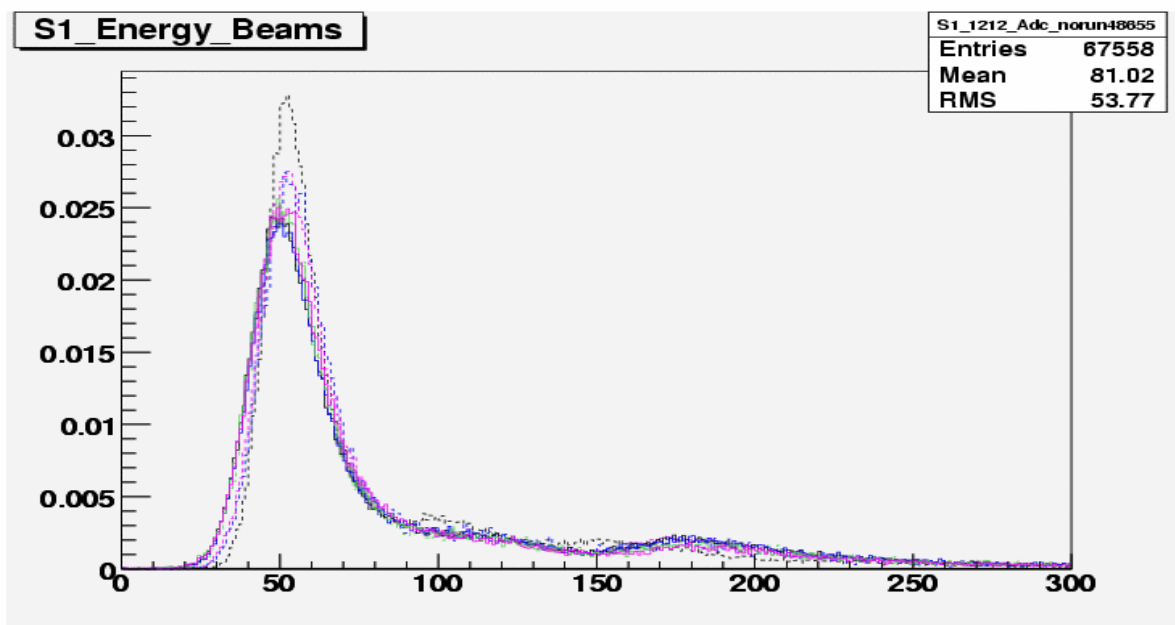


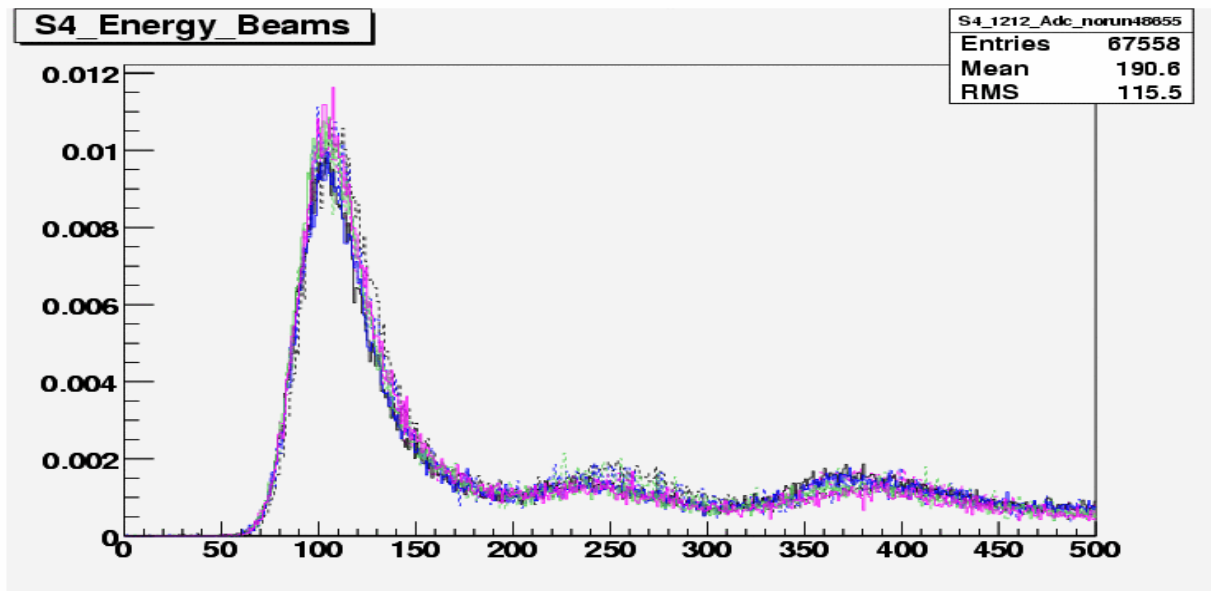
The results are about the same comparing wire chambers B and E. A miscalibration of the chamber could be a possible explanation. Another possible explanation is that the wire chamber B is located far from the others so beam optics effects become important while the relative distance between C and E is small and the effects can be neglected.



- *Scintilators: S1, S2 and S4*

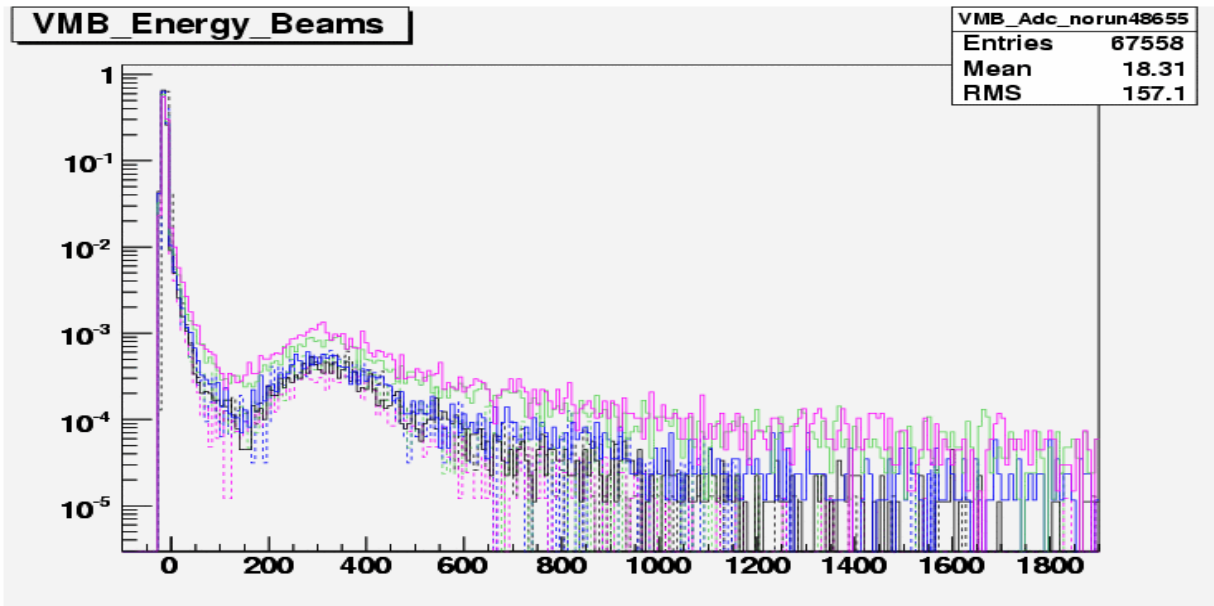
In the following histograms the response of the scintilators S1, S2 and S4 are presented. We notice that the behavior of the counter is the same for all the beams. One can distinguish zero-, one-, two- and three-hit contributions.





- *Muon counter: VMB*

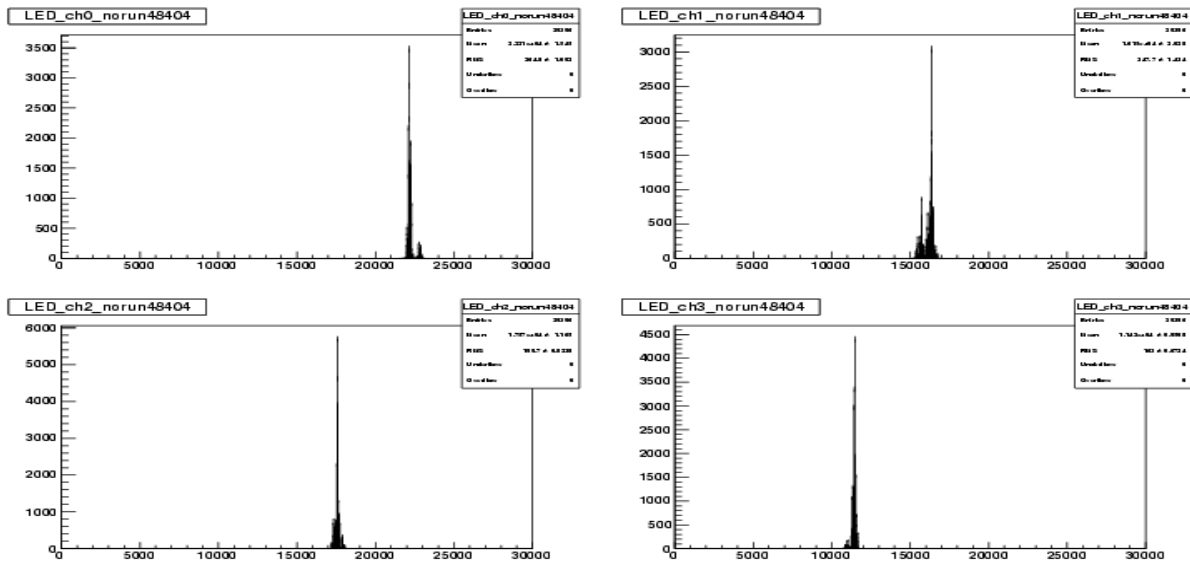
The response of the VMB counter is as expected (as shown in the following histogram). Higher muon admixture is observed at high electron beam energies.



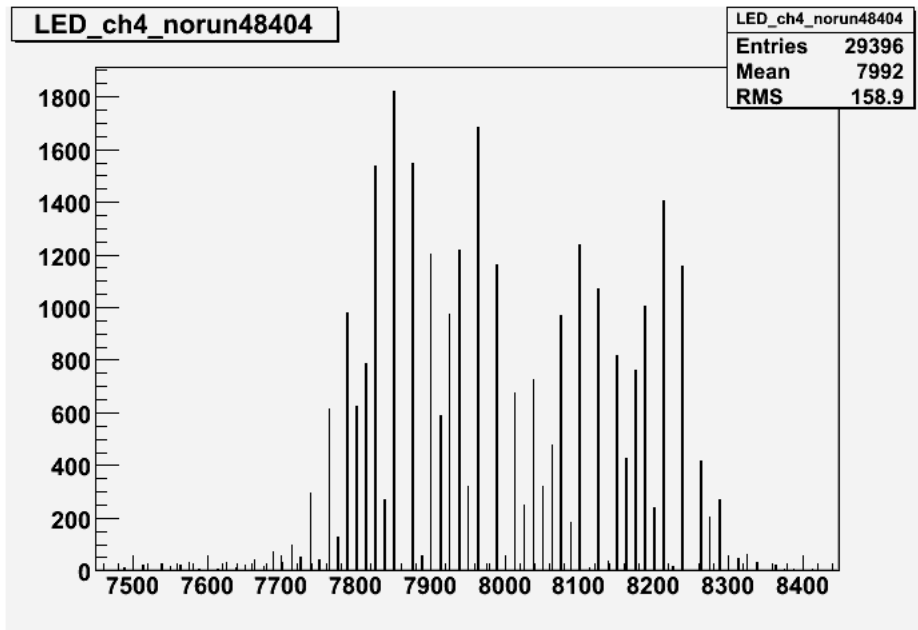
## LED analysis

- *LED amplitude distribution*

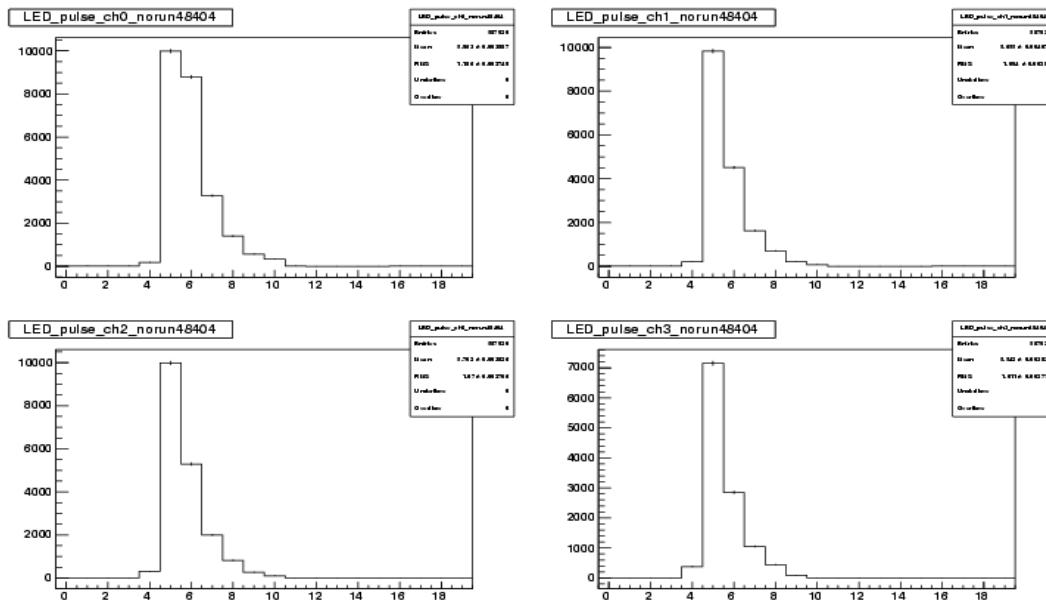
The LED (Light Emitting Diode) light was used to illuminate CASTOR photodetectors. The LED signal amplitude value is the sum of the amplitude of four time slices 4,5,6,7 for LED trigger events. The following histograms refer to run number 48404 and the 4 first saleve-side channels. We notice that the distributions are narrow peaks in a wide range.



However, if we look closely at the amplitude distribution of one channel (e.g. ch4) we see a discrete set of values. The step size of the ADC is quite big for the LED intensity chosen during the test beam and as a result the digitization leads to information loss.



In the following histograms the pulse shape of the LED signal is presented. The value of 10000 is the upper limit of the dynamic range of the CASTOR electronics. From the graphs we see that three of the four channels presented here are saturated.

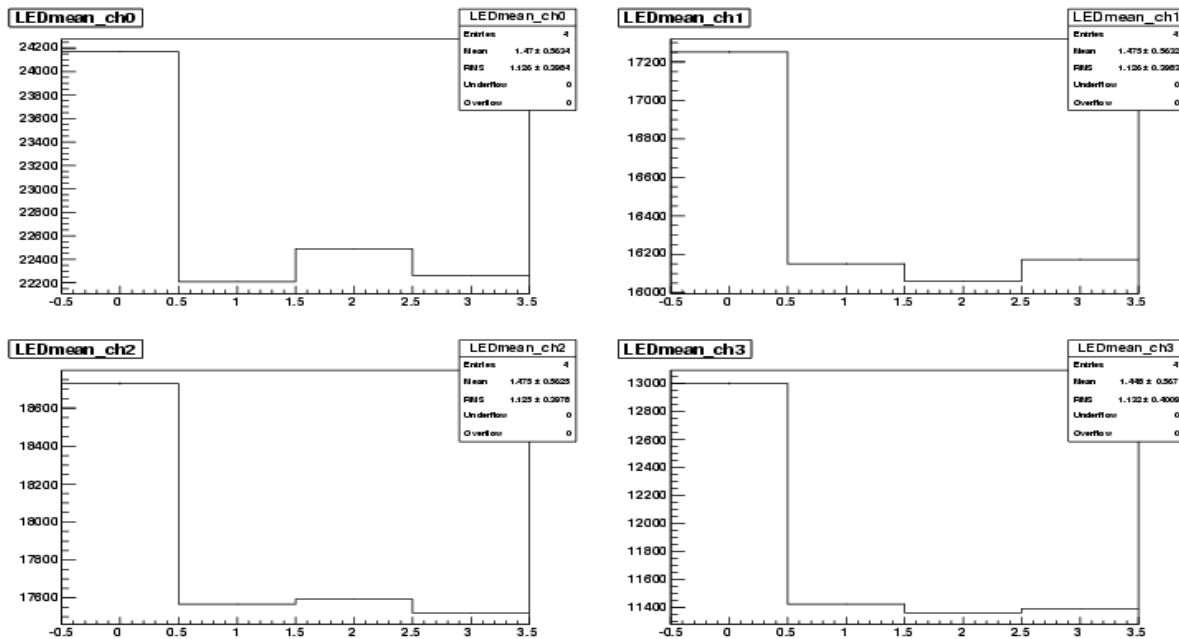


The overall conclusion is that for the final system the intensity should be decreased in order to make other studies feasible (e.g. gain studies).

- LED mean stability

In order to examine the LED amplitude mean value stability we compare the mean values over 4 different test runs. The runs studied along with corresponding time stamps are listed below:

- 47386 (16/6 19:43 )
- 48404 (23/6 13:01 )
- 48726 (25/6 16:50 )
- 48797 (26/6 10:11 )

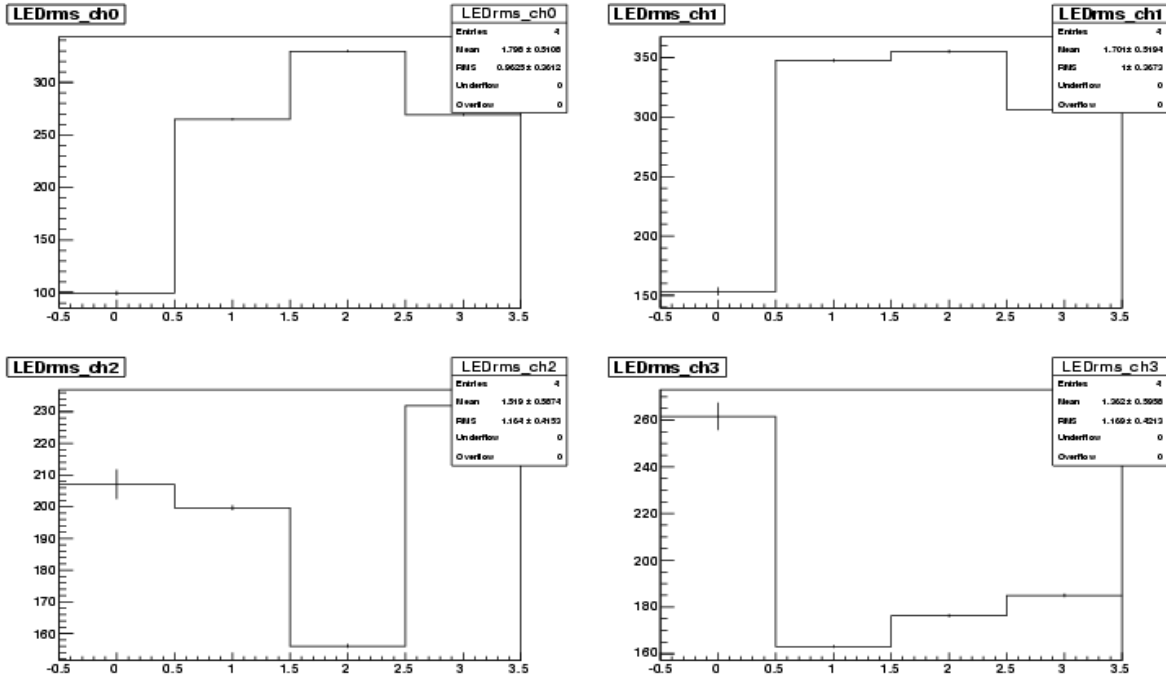


The variation of the mean values of the runs that were taken within three days is quite small while the mean value of the first run deviates stronger.

The conclusion therefore is that the mean values are quite stable in short term while we have a 10% variation in longer term.

- *LED RMS stability*

In addition to the mean stability we also examined the respective RMS stability. The RMS values, as it is obvious from the following graphs, are not stable. This is mainly because of the digitization effects. An other factor is that the first run has very low statistics, with big error bars and values different from the other runs.



# Conclusions

The overall conclusion from the pedestal analysis is that the pedestal mean and RMS are stable, so it is safe to say that the electronics performed well throughout the test beam.

We also studied the behavior of the beam counters for different energies. Concerning the wire chamber position reconstruction we found that a miscalibration of chamber B could explain the observed signals. Another possible explanation might be beam optic effects that become important only for chamber B because it is located relatively far from the others. The behavior of the other beam counters scintillators and muon counter, was as expected.

Concerning the LED signal analysis we found that the mean is quite stable in short term while for the long term the stability is at a level of 10%. The most important conclusion from the LED analysis is that the intensity has to be decreased because saturated channels were observed. In addition the ADC digitization step was too big for this intensity and the digitization leads to information loss. Therefore for the final system we need to lower the intensity to make other studies (e.g. gain studies) feasible.

## References

1. CMS CASTOR EDR 31 October 2007
2. CMS-ECAL TDR
3. Norbeck,E. et al,“Exotic Physics at the LHC with CASTOR in CMS”, CMS CR 2007/013
4. Aslanoglou,X. et al, “Performance studies of prototype 2 for the CASTOR calorimeter at the CMS experiment”,Eur. Phys. J. C52, 495-506(2007)
5. [//cmsdoc.cern.ch/castor/](http://cmsdoc.cern.ch/castor/)